# Development of a Trispecific Antibody Designed to Simultaneously and Efficiently Target Three Different Antigens on Tumor Cells

Nazzareno Dimasi,*,[†] Ryan Fleming,[†] Carl Hay,[‡] Rob Woods,[†] Linda Xu,[†] Herren Wu,[†] and Changshou Gao*,[†]

[†]Antibody Discovery and Protein Engineering and [‡]Oncology Research, MedImmune, Gaithersburg, Maryland 20878, United States

S *Supporting Information*
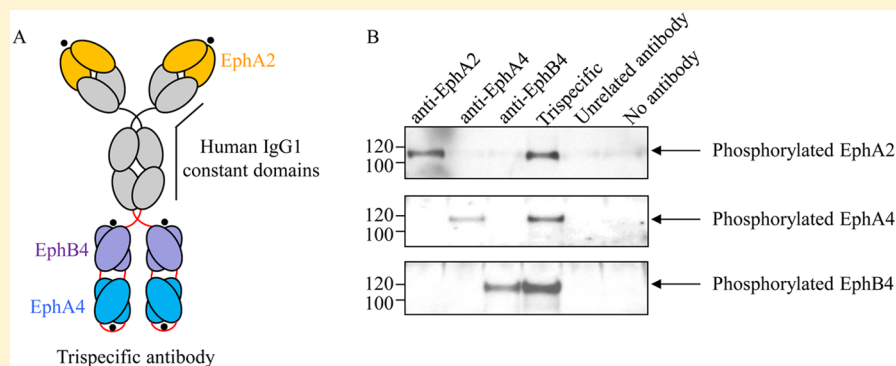
ABSTRACT: Targeting Eph (erythropoietin producing hepatoma) receptors with monoclonal antibodies is being explored as therapy for several types of cancer. To test whether simultaneous targeting of EphA2, EphA4, and EphB4 would be an effective approach to cancer therapy, we generated a recombinant trispecific antibody using the variable domain genes of anti-EphA2, anti-EphA4, and anti-EphB4 monoclonal antibodies. A multidisciplinary approach combining biochemical, biophysical, and cellular-based assays was used to characterize the trispecific antibody *in vitro* and *in vivo*. Here we demonstrate that the trispecific antibody is expressed at high levels by mammalian cells, monodispersed in solution, thermostable, capable of simultaneously binding the three receptors, and able to activate the three targets effectively as evidenced by receptor internalization and degradation both *in vitro* and *in vivo*. Furthermore, pharmacokinetic analysis using tumor-bearing nude mice showed that the trispecific antibody remains in the circulation similarly to its respective parental antibodies. These results indicate that simultaneous blockade of EphA2, EphA4, and EphB4 could be an attractive approach to cancer therapy.

KEYWORDS: *trispecific antibody, tumor targeting, EphA2, EphA4, EphB4, differential scanning calorimetry, analytical ultracentrifugation*

INTRODUCTION

Eph receptors (erythropoietin producing hepatoma) are the largest receptor tyrosine kinase family of transmembrane proteins with an extracellular domain capable of transducing signals from the outside cell environment to the inside compartments, thus influencing the growth and survival of cells directly by acting on gene transcription or indirectly by affecting the production of second messengers.[1,2] Eph receptors are divided into either type A or B, based on their interactions with ephrin ligands.[3] There are nine members of the A-type (EphA1−8 and EphA10) and five members of the B-type (EphB1−4 and EphB6). Among Eph receptors, EphA2, EphA4, and EphB4 are considered to be potential targets for anticancer therapies because of their high expression in a wide variety of human tumors and low expression levels in normal tissues.[4] EphA2 is overexpressed in several carcinomas including breast, lung, liver, gastrointestinal, prostate, esophageal squamous cell carcinoma, ovarian cancer, and melanoma;[5] EphA4 is overexpressed in prostate cancer, colon cancer, lung cancer, liver cancer, and melanoma;[6] EphB4 is abundantly expressed in several carcinomas including breast, liver, gastrointestinal, leukemia, prostate, lung, and melanoma.[7−13]

One key to successful cancer treatment is the use of combinatorial therapeutic regimens comprising several therapeutic agents.[14] This type of combination therapy has been proven to prolong survival, control disease progression, and improve quality of life without excessive toxicity.[14] Such therapy may include the use of a combination of different small molecule cytotoxic drugs or a combination of monoclonal antibodies and small-molecule chemotherapeutic drugs.[15−18] Yet another approach successfully used in the treatment of tumors is the combination of two or more monoclonal antibodies.[19−24]

The advantage of using monoclonal antibodies in cancer therapy is their exquisite specificity, therefore reducing toxicity, the

possibility to conjugate small molecule cytotoxic drugs, thereby increasing targeted delivery of the cytotoxic drugs, the possibility of targeting different epitopes on the same receptor, thus lowering the rise of tumor escape mutants, and the possibility to target tumor antigens that may be expressed at different stages of the cancer development, thus improving therapeutic efficacy.

Clinical application of combinatorial antibody therapy is hindered by a multitude of factors, primarily by problems related to the development, production, and subsequently high regulatory costs of each individual antibody.[25] An alternative approach to overcome these problems is to combine the binding domains of two or more antibodies with different specificities by means of antibody engineering, thus creating polyspecific antibodies.[26] Polyspecific antibodies are a class of biological drugs engineered to simultaneously bind two or more target antigens.

We have established an antibody technology platform that allows rapid and efficient engineering of multiple binding sites in a single molecule.[27,28] Expanding upon our technology we report herein the construction and characterization of a trispecific antibody capable of simultaneously binding to three different antigens (EphA2, EphA4, and EphB4), which are broadly overexpressed on tumor cells. By employing a multidisciplinary approach, we demonstrated that this trispecific antibody is highly expressed in mammalian cells, monodispersed in solution, thermostable, capable of simultaneously binding its three target antigens, possesses pharmacokinetic properties similarly to its parental antibodies, and last, but most importantly, has potent *in vitro* and *in vivo* activity.

■ EXPERIMENTAL SECTION

Reagents and Cells Lines. All chemicals used were of analytical grade. Restriction enzymes and DNA-modifying enzymes were purchased from New England Biolabs. Oligonucleotides were purchased from Life Technologies. *Escherichia coli* Stbl3 cells used for plasmid amplification were purchased from Life Technologies. Protein expression was carried out using FreeStyle 293-F cell (Life Technologies). MIA PaCa-2 (human pancreatic carcinoma cell line) and PC-3 (human prostate adenocarcinoma cell line) cells were used for FACS, internalization, receptor activation, and *in vivo* analyses.

Construction, Expression, and Purification of the Trispecific and Parental Antibodies. Preparation of the trispecific antibody was carried out using molecular biology methods as described by Dimasi et al.[27] Briefly, the VH of the anti-EphB4 was linked to the VL of the anti-EphA4 using a GGGGS linker; this DNA fragment was linked to the VH of the anti-EphA4 using a $(GGGGS)_4$ linker, and finally this DNA fragment was linked to the VL of the anti-EphB4 using a GGGGS linker. The final DNA fragment consisting of the anti-EphB4 and anti-EphA4 binding domains was linked to the C-terminal domain of the anti-EphA2 heavy-chain antibody using a AAAGGGGS linker. The amino acid sequence of the trispecific antibody is shown in Supplementary Figure 1. The parentals (anti-EphA2, anti-EphB4, and anti-EphA4), negative isotype control (R347), and trispecific antibodies were expressed and purified as described by Dimasi et al.[27] The purified proteins were then analyzed on a 12% SDS-PAGE under nonreducing and reducing conditions, followed by Coomassie brilliant blue (Bio-Rad) staining.

ELISA and Flow Cytometry. Single and dual antigen binding ELISA assays were carried out essentially as described by Dimasi et al.[27] Briefly, for the single antigen binding assay, 2 μg/mL of antigens (human EphA2-FLAG and human EphA4-Fc

produced at MedImmune; and human EphB4-Fc-His purchased from R&D Systems) were coated on ELISA plates. Serial dilution of the trispecific antibody was added, and detection was carried out using an antihuman-Fc HRP conjugate (R&D Systems). Dual ELISA binding was carried out by direct immobilization of the first antigen, followed by a serial dilution of the trispecific and addition of the second antigen. Detection was carried out using an anti-FLAG HRP conjugated antibody for the dual binding to EphA4-EphA2 and EphB4-EphA2, respectively. For the dual binding to EphA2-EphB4 an anti-His HRP conjugated antibody was used for detection. Flow cytometry was used to assess the binding capacity of the parental antibodies and the trispecific antibody to human pancreatic carcinoma cells (MIA PaCa-2), which express EphA2, EphA4, and EphB4. Cells were grown in DMEM with 10% FBS and detached using Accutase (e-Bioscience). Cells were washed and resuspended in 1% BSA and 0.1% NaN_3 in PBS. A total of 100 μL of cells at 1×10^6 cells/mL were dispensed into a 96 well microplate. All antibodies used were biotinylated using NHS-PEG4-Biotin (Thermo Fisher Scientific) following manufacturer's protocol. The cells were then incubated at 4 °C for 1 h with their respective biotinylated antibodies (trispecific, anti-EphA2, anti-EphA4, anti-EphB4, and R347) at a concentration of 1 μg/mL. After washing with 1% BSA in PBS, the cells were stained with Streptavidin-Alexa fluor 488 (Life Technologies). Cell-associated fluorescence was analyzed with Guava flow cytometry (EMD Millipore) and plotted using the program FlowJo (http://www.flowjo.com). For competition binding experiments, EphA2 and EphB4 (20 μg/mL) and EphA4 (10 μg/mL) were preincubated with the trispecific antibody (1 μg/mL) for 1 h at 4 °C.

Surface Plasmon Resonance Measurements. Binding experiments were carried out using a BIAcore 3000 instrument (BIAcore). Preliminary test binding experiments (data not shown) indicated that stable binding (i.e., slow dissociation) was observed when EphA2-FLAG was immobilized on the BIAcore sensor chip. EphA2 immobilization was performed at a flow rate of 10 μL/min using standard amino coupling. Briefly, the CM5 sensor chip surfaces were activated with a 1:1 mixture of 1-ethyl-3-(3-(dimethylamino)propyl)-carbodiimide (EDC) and *N*-hydroxysuccinimide (NHS). EphA2-FLAG was prepared at 1 μM in 10 mM sodium acetate (NaOAc), pH 4, and then injected over the activated flow cell surface. Following this, unreacted active sites were capped by injecting 1 M solution of ethanolamine over the surface. Separately, a blank surface was also prepared on each chip using the identical coupling protocol minus the EphA2-FLAG ligand. This blank surface was used as a reference cell throughout the experiments and served to correct for nonspecific binding. EphA2-FLAG was immobilized at a density of about 3000 response units (RU). A flow rate of 75 μL/min was used for the test-binding measurements. For the concurrent binding experiments, the trispecific, R347, EphA4, and EphB4 were prepared at 500 nM in 10 mM HEPES buffer, 150 mM NaCl, 3 mM EDTA, and 0.005% Tweeen-20, pH 7.4, and sequentially injected over EphA2-FLAG and control surfaces. The earlier antigens were included in the mixture for subsequent injections to ensure saturation binding of the earlier antigens during the concurrent binding. Between injections, the EphA2-FLAG surface was regenerated with 1 min injection of 50 nM NaOH containing 1 M NaCl. The fully corrected data were then generated using the BIAevaluation 4.1 software (GE Healthcare, Pittsburgh, PA), and the figure was prepared using Prism 5 software.

Analytical Ultracentrifugation. Sedimentation equilibrium studies were carried out using a Beckman ProteomeLab

XL-A analytical ultracentrifuge equipped with absorbance optics (Beckman Coulter, Indianapolis, IN). Both parental and trispecific antibodies were analyzed in PBS pH 7.4 and purified by gel-filtration before loading into the analytical ultracentrifuge. Sedimentation equilibrium was attained at a rotor temperature of 25 °C and at a rotor speed of 42 000 rpm. Absorbance versus radius scans were acquired in 0.002 cm radial increments at 280 nm. The distribution of molecular species (i.e., amounts of material sedimenting at different rates) was obtained using the program SedFit.[29]

Differential Scanning Calorimetry. Differential scanning calorimetry (DSC) experiments, data analysis, and evaluation were carried out using the same procedures as described by Dimasi et al.[27]

Antibody Internalization. PC-3 cells were added to a 96 well U bottom plate at 1×10^6 cells per well. The cells were washed twice with PBS and labeled with 5 μg of the control, parental, or trispecific antibodies for 30 min on ice. Cells were then washed twice with PBS and incubated with growth media at 37 °C for 0, 10, 20, 30, and 60 min. The cells were then fixed in 3.7% paraformaldehyde for 20 min, washed twice in PBS, and permeabilized using 0.5% Triton X-100 in PBS for 5 min at room temperature. The cells were again washed twice with PBS and labeled with 1 μg of AlexaFluor-488 goat-μ-human IgG antibody (Life Technologies). The excess secondary antibody was removed using two washes with cold PBS. The cells were spun onto a coated slide and mounted with a coverslip with Vectasheild Hardset mounting medium with DAPI (Vector Laboratories,). Internalization was analyzed by confocal laser-scanning microscopy at 63× magnification using a Leica SP5 microscope.

In Vitro Receptor Activation Assay. MIA PaCa-2 cells, which express EphA2, EphA4, and EphB4, were plated on a 6-well plate at 1×10^6 cells/mL in DMEM (Life Technologies) supplemented with 10% FBS and incubated for 2 days at 37 °C in a humidified atmosphere containing 5% CO_2. The cells were then washed with cold PBS and incubated with parental antibodies (anti-EphA2, anti-EphA4, and anti-EphB4) and trispecific antibody at 10 μg/mL for 30 min at 37 °C. An unrelated antibody (R347) and no antibody treatments were used as negative controls. After incubation the cells were washed twice with cold PBS and lysed using 200 μL of lysis buffer (50 mM Tris-HCl pH 7.4, 150 mM NaCl, 5 mM EDTA, 1% Triton X-100, 0.1% aprotinin, 0.1% leupeptin, and 0.1% Na-vanadate) for 5 min at room temperature. The lysate was collected in an eppendorf tube, and cellular debris were removed by centrifugation at 10 000 rpm for 5 min. Total protein concentration was determined using the BCA method (Thermo Fisher Scientific). Receptor immunoprecipitation was carried out using 50 μL of streptavidin magnetic beads (Life Technologies) coupled with biotinylated anti-EphA2 (MedImmune), anti-EphA4 (Life Technologies), and anti-EphB4 (MedImmune) at 5 μg/mL. The captured antibodies were washed twice using PBS and 0.1% Tween-20. Protein (120 μg in total) was incubated with the immobilized antibodies for 2 h at 4 °C under gentle rotation. After three washes with cold lysis buffer, the samples were resuspended in Laemmli SDS sample buffer and incubated for 10 min at 95 °C, and the supernatant was loaded on 10% NuPAGE bis-tris gels (Life Technologies). Following electrophoresis, the gels were washed with water and then transferred on PVDF membranes (Life Technologies). The membranes were washed with water and blocked for 1 h at room temperature with blocking buffer (30% Cold Fish Gelatin purchased from

Sigma-Aldrich), 0.1% BSA, and 0.1% Tween-20 in TBS buffer. The membranes were then incubated for 1 h at room temperature with an antiphosphotyrosine antibody 4G10 HRP conjugate (EMD Millipore) diluted 1:1000 in TBS buffer. After extensive washes with TBS, specific receptor phosphorylation was detected by enhanced chemiluminescence (ECL) as recommended by the manufacturer (Thermo Fisher Scientific).

In Vitro Degradation of EphB4 and EphA2. PC-3 cells were purchased from the American Type Culture Collection and maintained in F-12 Kaighn's media (Life Technologies) supplemented with 10% heat inactivated Fetal Bovine Serum (Life Technologies). Cells were maintained at 37 °C in a humidified atmosphere containing 5% CO_2. For the degradation assay, PC-3 cells were plated at 3×10^5 cells per well in 6-well plates (Falcon), incubated overnight, and treated with the trispecific antibody or control antibodies at 66.7 nM. One set of treated samples was harvested at 4 h for analysis of EphB4 degradation, and another set of treated samples was harvested at 24 h for analysis of EphA2 degradation. Cells were harvested by carefully removing the treatment media and adding 100 μL of ice cold 1% Triton-lysis buffer (Boston Bioproducts) containing 25 μg/mL Aprotinin (Sigma-Aldrich) and 10 μg/mL Leupeptin (Sigma-Aldrich). The plates were rocked for 5 min at 4 °C, and the lysates were collected and centrifuged at 10 000 rpm for 5 min at 4 °C. The supernatants were then collected, and the total protein concentration was determined using BCA Protein Assay kit (Thermo Fisher Scientific). For western-blot analysis, 20 μg of total protein was loaded onto a 10% bis-tris gel (Life Technologies) and probed with an anti-EphA2 antibody (Life Technologies) or an anti-EphB4 antibody (MedImmune). A peroxidase conjugated goat antimouse antibody (Jackson ImmunoResearch) was used as the secondary antibody. Protein bands were visualized by chemiluminescence using ECL Western Blotting Substrate (Thermo Fisher Scientific) and exposing to Kodak film. Similarly, the Western blot PVDF membranes were also probed for GAPDH (Glyceraldehyde 3-phosphate dehydrogenase) using an anti-GAPDH antibody (Cell Signaling Technology).

Pharmacodynamic (PD) and Pharmacokinetic (PK) Analysis. PC-3 prostate adenocarcinoma cells were implanted subcutaneously in the right flank of 7-week old nude mice (Harlan Sprague−Dawley) with 5×10^6 cells per mouse. Tumors were allowed to progress to approximately 100 mm³ before dosing with the trispecific antibody at 16.6 mg/kg body weight or the parental anti-EphA2 or anti-EphB4 antibodies at 10 mg/kg body weight. Tumors and serum were collected from three mice per time point per dose group at 0, 1, 4, 8, 24, 48, 72, 120, and 144 h postdose. Tumors and serum were collected from three mice, dosed with PBS, were harvested immediately after dosing (0 h). Tumors and serum were stored at −80 °C prior to processing. Tumors were homogenized in 1% Triton-lysis buffer containing 25 μg/mL Aprotinin and 10 μg/mL Leupeptin for 30 s in Lysing Matrix A tubes (MP Biomedicals) on a Fast Prep 24 System (MP Biomedicals). The lysates were centrifuged at 10 000 rpm for 5 min at 4 °C, and the supernatants were collected and analyzed for protein concentration by BCA (Thermo Fisher Scientific). Proteins (30 μg in total) from the tumor supernatants were loaded onto a 10% bis-tris gel and analyzed by Western blot for EphA2, EphB4, and GAPDH levels. The protein bands were quantified by densitometry analysis and normalized to the single protein band from the 0 h time point PBS control present on each of the three blots. The serum
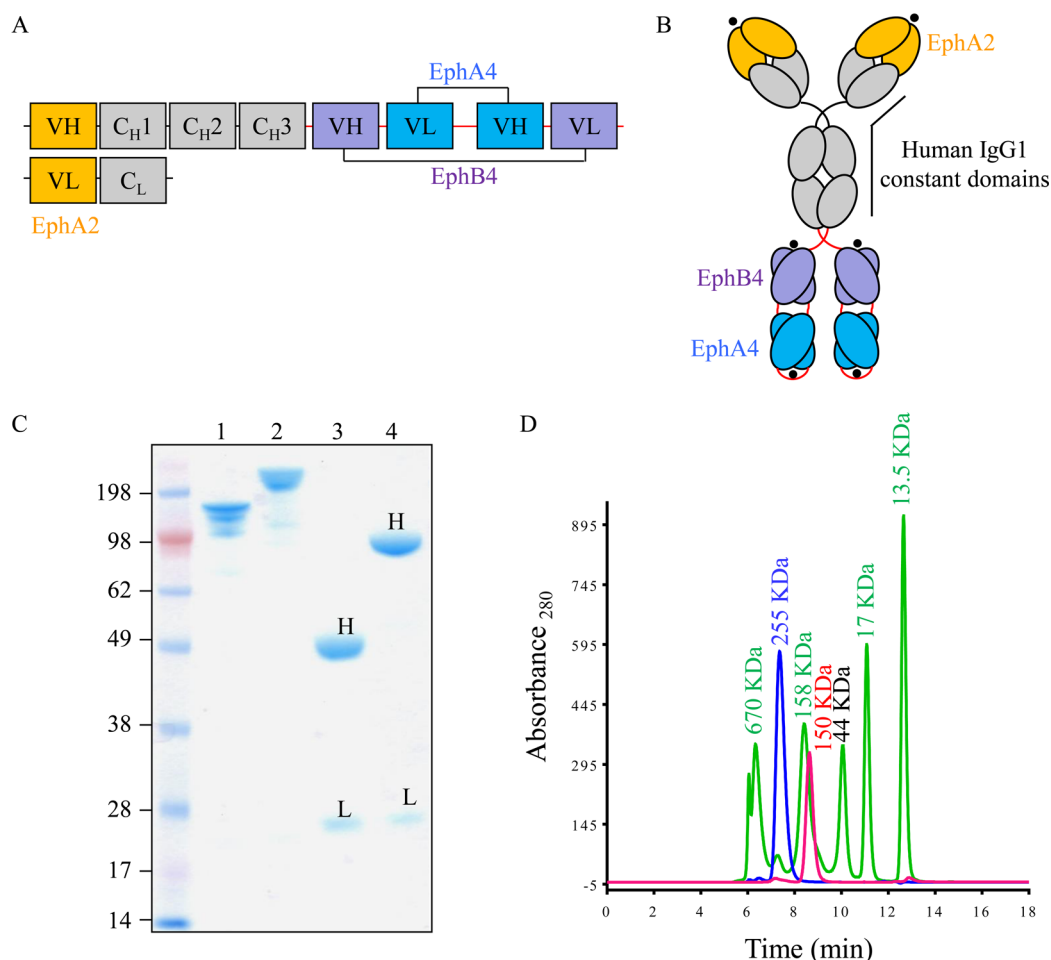
Figure 1. Schematic representation of the trispecific antibody, SDS-PAGE and SEC-HPLC analyses. (A) Domain organization and diagram illustration (B) of the trispecific antibody generated in this study. Domain and antigen specificities of the trispecific antibody are schematically labeled. The antigen binding sites in the cartoon representation of the trispecific antibody are indicated using black colored circles. (C) SDS-PAGE analysis of protein A purified trispecific antibody under nonreducing (line 2) and reducing conditions (line 4). The parental antibody anti-EphA2 is also shown under nonreducing (line 1) and reducing conditions (line 3). The light and heavy chains under reducing conditions (line 3 and 4) are denoted with L and H, respectively. The molecular mass standards are shown. (D) Size-exclusion HPLC chromatography of the trispecific antibody (blue chromatogram) after purification by preparative gel-filtration and of the parental anti-EphA2 antibody (red chromatogram). Peak positions of molecular weight protein standards (green chromatogram), trispecific (255 kDa), and parental antibody (150 kDa) are schematically labeled.

samples were analyzed for the presence of either trispecific antibody or parental anti-EphA2 or anti-EphB4 control antibodies using an EphA2 or EphB4 binding ELISA. Maxisorp ELISA 96-well plates (Sigma-Aldrich) were coated with either human EphA2 or EphB4 at 5 μg/mL in PBS pH 7.4, overnight at 4 °C. Plates were blocked with 4% nonfat dry milk and then washed with 0.1% Tween-20 in PBS. Serum samples (diluted 1:1000) were loaded and incubated for 1 h at 22 °C. For both the EphB4 and EphA2 binding ELISA, standard curves were prepared with serial dilutions of purified protein from 1 μg/mL to 10 ng/mL. The HRP conjugated secondary antibodies used were goat-antimouse (ImmunoResearch) for the anti-EphB4 control antibody ELISA. The HRP conjugated secondary antibody used for both the anti-EphA2 control antibody and trispecific antibody EphA2 ELISA was goat-antihuman (Jackson ImmunoResearch). The procedures described in this study were performed humanely under a protocol approved by MedImmune Institutional Animal Care and Use Committee in a facility accredited by AAALAC International (http://www.aaalac.org/).

■ RESULTS

Design, Expression, and Purification of the Trispecific Antibody. The trispecific antibody was constructed by linking a diabody anti-EphB4/anti-EphA4 to the carboxyl-terminus C_H3 domain of an anti-EphA2 antibody. As shown in Figure 1A, the V-domains of the diabody are in the orientation VH_{EphB4}-Linker-VL_{EphA4}-Linker-VH_{EphA4}-Linker-VL_{EphB4}. The VH_{EphB4}-VL_{EphA4} and VH_{EphA4}-VL_{EphB4} are linked by a short five-amino-acid linker (Gly-Gly-Gly-Gly-Ser), which restricts intrachain pairing of the VH_{EphB4}-VL_{EphA4} and VH_{EphA4}-VL_{EphB4}. A 20-amino-acid linker (Gly-Gly-Gly-Gly-Ser)$_4$ was used to link the VL_{EphA4}-VH_{EphA4}. The EphB4 and EphA4 diabody was linked to the C-terminus of the anti-EphA2 antibody using a linker with sequence Ala-Ala-Ala-Gly-Gly-Gly-Gly-Ser. The amino acid sequence of the trispecific antibody is shown in Supplementary Figure 1. A cartoon representation of the trispecific antibody is shown in Figure 1B, which shows potential domain orientation of the diabody with binding sites of the trispecific antibody indicated by black colored circles.

The trispecific antibody and parental antibodies were transiently expressed in 293-F cells, which resulted in expression
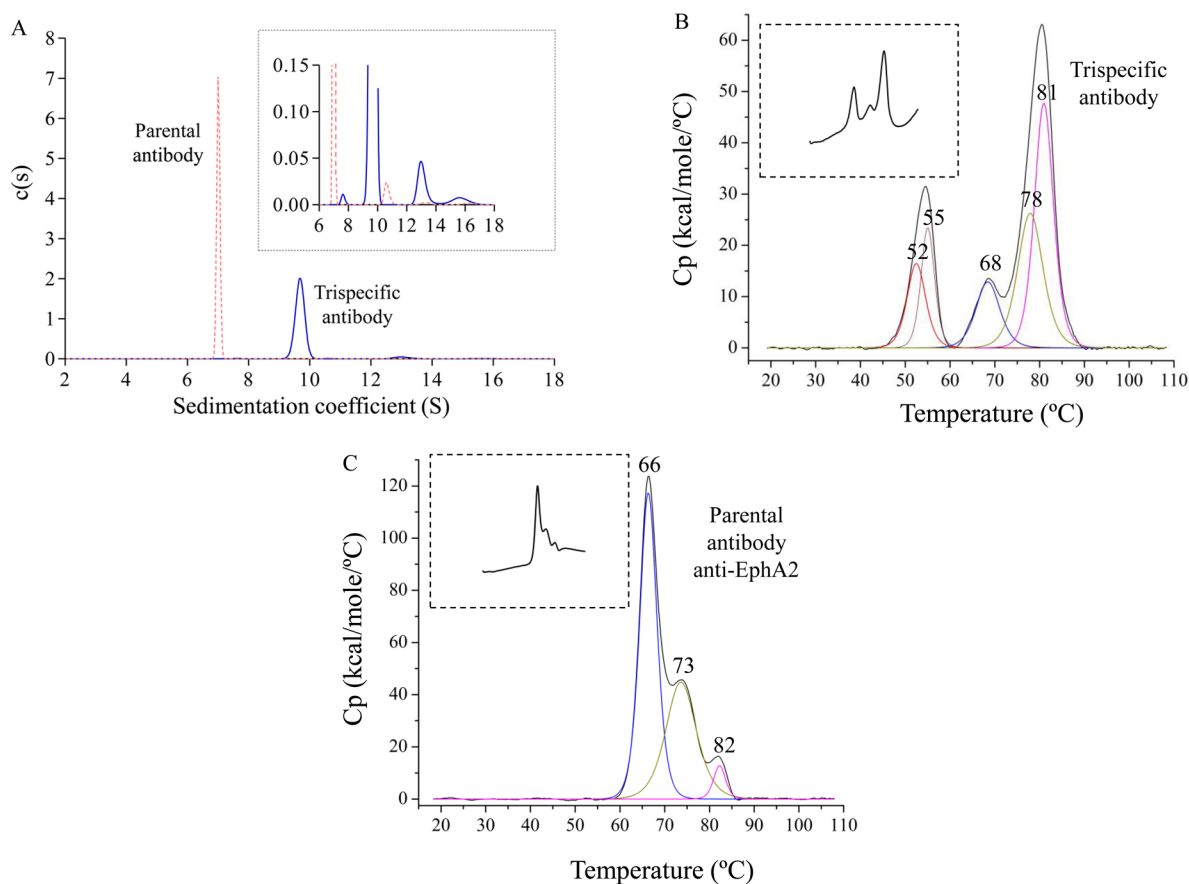
Figure 2. Size-distribution analysis and thermostability of the trispecific antibody. (A) Normalized sedimentation coefficient distribution plot for the trispecific (blue curve) and anti-EphA2 parental antibody (red-dashed curve). The inset shows the same coefficient distribution plot for trispecific and parental antibodies at an expanded vertical scale (magnification 55×) so the minor (<3%) aggregate and fragment components can be seen. The size distribution analysis revealed that the trispecific antibody exists in solution as a major monodisperse form (97% monomeric) with a sedimentation coefficient of 9.8 S. As a comparison, the parental antibody has a sedimentation coefficient of 7.1 S, which correspond to ~98% of the sample. Thermal unfolding transitions for the trispecific (B) and anti-EphA2 parental (C) antibodies obtained by differential scanning calorimetry (DSC). The black curves represent the experimental baseline subtracted and concentration normalized endothermic transitions, while the other curves represent the respective non-two-state transitions obtained by deconvolution analysis of the excess heat capacity. These curves are color coded such as the deconvolution transition for the anti-EphA4 domain is red, the anti-EpB4 is orange, the C_H2 domain is blue, the Fab domain is gold, and the C_H3 domain is magenta. Experimental endothermic curves normalized for concentration are shown as black lines in the insets in both panels C and B.

levels of about 100 mg/L. The trispecific and parental antibodies were purified by standard protein A affinity chromatography and analyzed by reducing and nonreducing SDS-PAGE (Figure 1C). The SDS-PAGE relative mobility of the purified proteins under reducing conditions were consistent with the expected molecular masses of about 25 kDa for the light chains of both the parental and trispecific antibodies (Figure 1C, lines 3 and 4, lower bands), of about 50 kDa for the parental antibody heavy chain (Figure 1C, line 3, upper band), and of about 100 kDa for the trispecific heavy chain (Figure 1C, line 4, upper band).

After protein A purification, the trispecific antibody was analyzed by analytical SEC-HPLC, which revealed that 40% (data not shown) of the affinity purified trispecific antibody was forming soluble high-molecular weight aggregates. The monomer was separated from the aggregate using preparative gel-filtration chromatography and reanalyzed by analytical gel-filtration chromatography (Figure 1D), showing that the purified trispecific was 98% monomer. Furthermore, the monomeric form eluted from the gel-filtration column had its expected molecular weight of 255 kDa with a retention time of 7.7 min (Figure 1D, blue chromatogram). This value is in agreement with the intact molecular weight determined using mass spectrometry

(data not shown). As a comparison, the retention time for the parental antibody anti-EphA2 was 8.6 min (MW 150 kDa; Figure 1D, red-dashed chromatogram).

Sedimentation Velocity and Thermostability. The trispecific and parental anti-EphA2 antibodies were analyzed by sedimentation velocity to determine their monodispersity and by differential scanning calorimetry (DSC) to determine their thermostability. Monodispersity and thermostability are indications of manufacture feasibility. Figure 2A shows the normalized sedimentation distribution plot at pH 7.4 for the trispecific antibody (blue curve) and for the parental anti-EphA2 antibody (red-dashed curve). The main peak of the trispecific antibody, corresponding to the monomer, has a sedimentation coefficient of 9.8 S (Svedberg) and represents 97% of the sample. For comparison, the main peak for the parental anti-EphA2 antibody has a sedimentation coefficient of 7.1 S corresponding to 98% of the sample. There are also minor peaks (<3%) present for both the trispecific and parental antibody samples, more clearly seen in a 55-fold expanded plot of the sedimentation velocity (inset to Figure 2A). Based on their sedimentation coefficients, these peaks presumably correspond to unidentified fragments, dimers, and trimers.

As shown by differential scanning calorimetry (DSC) analysis, the trispecific antibody undergoes endothermic unfolding at pH 6.0 with three transition peaks (Figure 2B and inset). These observed endothermic transitions are typical for polyspecific antibodies.[27] The three endothermic transitions can be further deconvoluted into five distinct endothermic unfolding transitions with a T_m of 52, 55, 68, 78, and 81 °C. By comparing the deconvoluted unfolding transitions for the parental anti-EphA2 antibody (Figure 2C and inset) and the individual scFv-Fc,[27] the five deconvoluted transition peaks for the trispecific antibody can be assigned to the unfolding of the scFv anti-EphA4 (T_m of 52 °C), the scFv anti-EphB4 (T_m of 55 °C), the antibody C_H2 domain (T_m of 68 °C), the antibody Fab domain (T_m of 78 °C), and finally the antibody C_H3 domain (T_m of 81 °C).
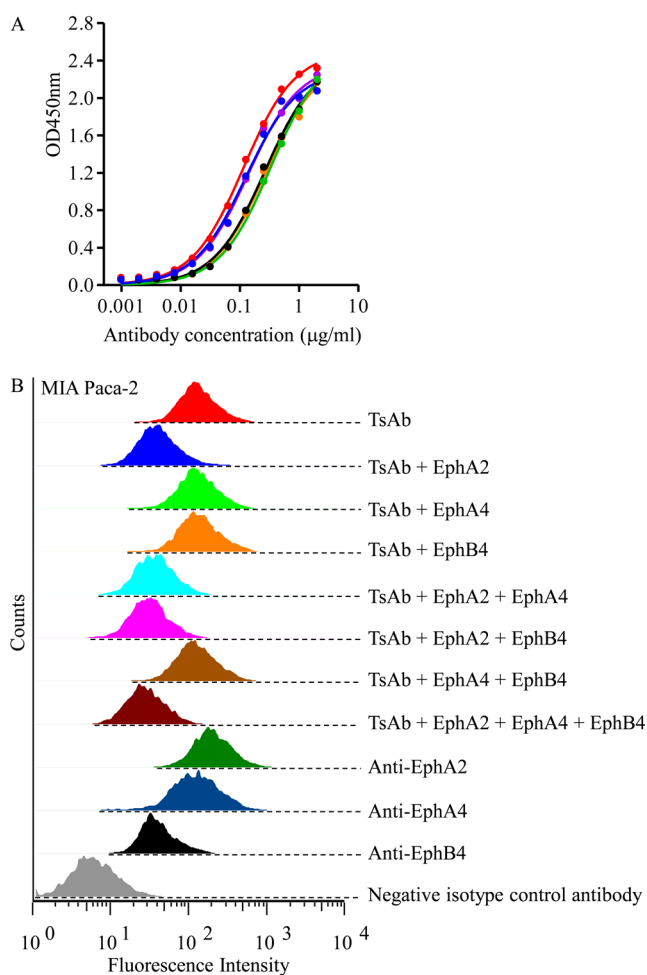
Concurrent Binding of the Trispecific Antibody to Its Antigens. A number of independent but complementary assays, using recombinant or membrane bound antigens, were used to assess the binding of the trispecific antibody to its antigens. ELISA was used to access the binding of the trispecific antibody to individual or simultaneous pairs of antigens. FACS was used to determine binding of the trispecific to cell surface antigens; and BIAcore was used to test the simultaneous binding to all three antigens. ELISA binding assay showed the trispecific antibody binds individually to EphA2, EphA4, and EphB4 (Figure 3A, blue, red, and green curves) and engages pairs of them simultaneously. For instance, the trispecific antibody simultaneously binds to EphA2 and EphA4 (Figure 3A, orange curve); to EphA2 and EphB4 (Figure 3A, black curve); and to EphA4 and EphB4 (Figure 3A, violet curve). These experiments show that there is no steric hindrance in the binding of the trispecific to the three antigens and more importantly the diabody binds to its cognate EphA4 and EphB4 antigens.

The binding to cell surface antigens was analyzed by FACS using pancreatic carcinoma cells (MIA PaCa-2) that express EphA2, EphB4, and EphA4. As shown in Figure 3B, the trispecific antibody efficiently binds to MIA PaCa-2 cells, and this binding is specifically blocked or diminished by incubating the trispecific antibody with the three recombinant antigens. The negative control antibody (R347) and the three parental antibodies, anti-EphA2, anti-EphB4, and anti-EphA4, were used as controls. The variability in the blocking experiments (Figure 3B) may be due to different levels of antigen expression by the MIA PaCa-2 cells.

BIAcore analysis was used to determine the simultaneous binding of the trispecific antibody to EphA2 and EphA4, to EphA2 and EphB4, and to the three antigens.

Preliminary test binding experiments (data not shown) suggested that best binding responses are obtained when EphA2 is immobilized on the BIAcore sensor chip. Figure 4A shows that the trispecific binds concurrently to EphA2 and EphA4; and Figure 4B shows that the trispecific binds concurrently to EphA2 and EpB4. Next, we determined that the trispecific binds concurrently to the three antigens. In fact, using the EphA2 surface, the trispecific binds to EphA2, to EphA4, and to EphB4 (Figure 4C), and the concurrent binding is retained when the order of the last antigens is reverted EphB4 before EphA4 (Figure 4D). These experiments show that the trispecific binds concurrently to its cognate antigens irrespective of sequence of binding events. Figure 4D shows that binding to antigens is not detected when the isotype control antibody (R347) is used.

Cellular Internalization of the Trispecific Antibody. To confirm cellular uptake of the trispecific and parental anti-EphA2
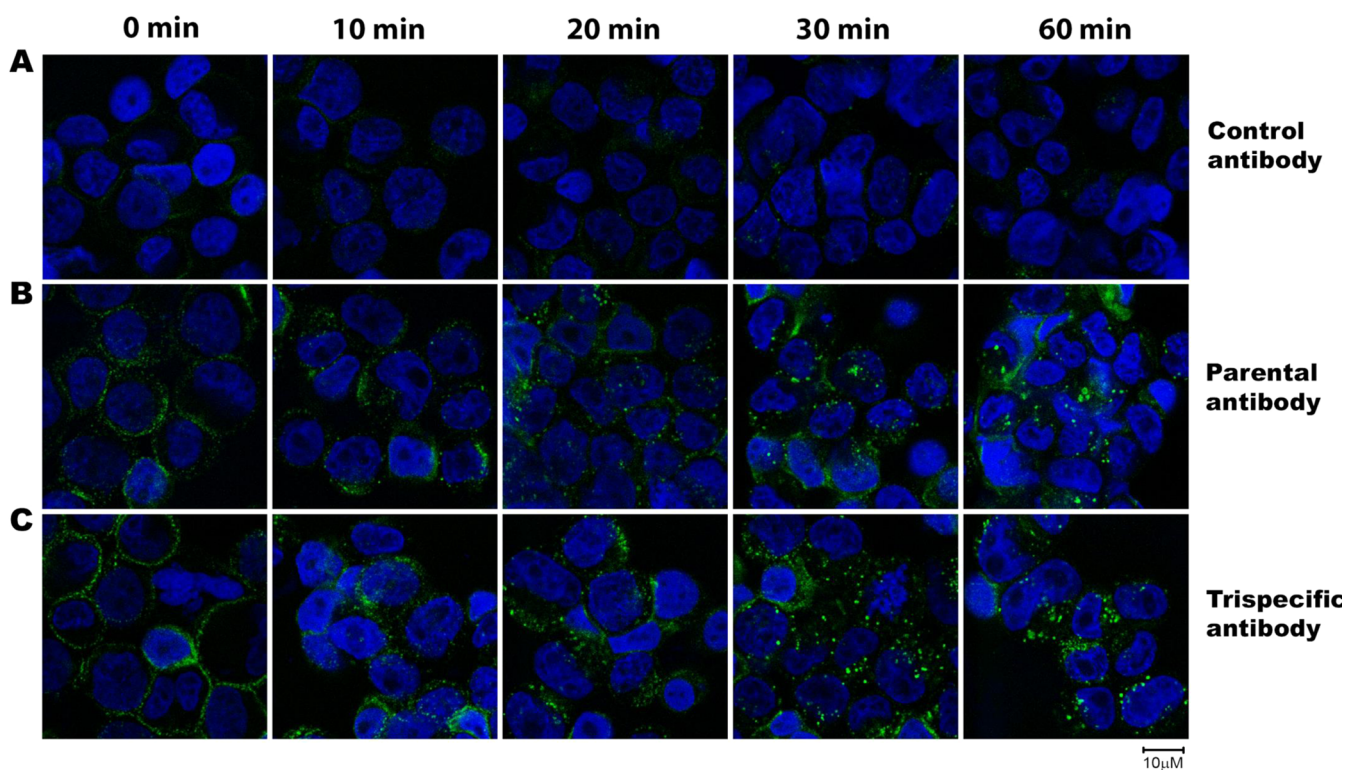

Figure 3. Binding analysis of the trispecific antibody (TsAb) determined using ELISA and FACS. (A) The binding of the trispecific antibody to EphA2, EphA4, and EphB4 antigens is shown in blue, red, and green, respectively. The simultaneous binding to EphA2 and EphA4 is shown in orange, the simultaneous binding to EphA2 and EphB4 is shown in black, and the concurrent binding to EphA4 and EphB4 is shown in violet. ELISA analysis revealed that the trispecific antibody is able to bind to its individual antigens and simultaneously engage pairs of antigens. (B) Flow cytometry was used to assess the binding capacity of the trispecific antibody to the cell surface antigens (EphA2, EphA4, and EphB4) expressed on MIA PaCa-2 pancreatic carcinoma cells. The cells were incubated with their respective antibodies as shown and specific binding was visualized. The FACS binding assay showed that the trispecific antibody binds to its cognate antigens expressed on the cell surface. The binding of the trispecific antibody is decreased upon preincubation of the trispecific antibody with recombinant antigens.

antibodies, MIA PaCa-2 tumor cell lines, which express all three target receptors (EphA2, EphA4, and EphB4), were incubated with the trispecific antibody, parental anti-EphA2, and negative control R347 antibody for 0, 10, 20, 30, and 60 min at 37 °C at a concentration of 5 μg/mL to allow receptor-mediated internalization. Receptor-mediated internalization was detected via fluorescently labeled anti-Fc antibody using confocal laser-scanning microscopy. Positive internalization was characterized by bright fluorescence within the cell cytoplasm, together with a decrease in membranous (extracellular) fluorescence. As seen in Figure 5B,C, the parental anti-EphA2 and trispecific antibodies were rapidly internalized after 10 min as shown by the intracellular staining (green fluorescent color) with a pattern typical
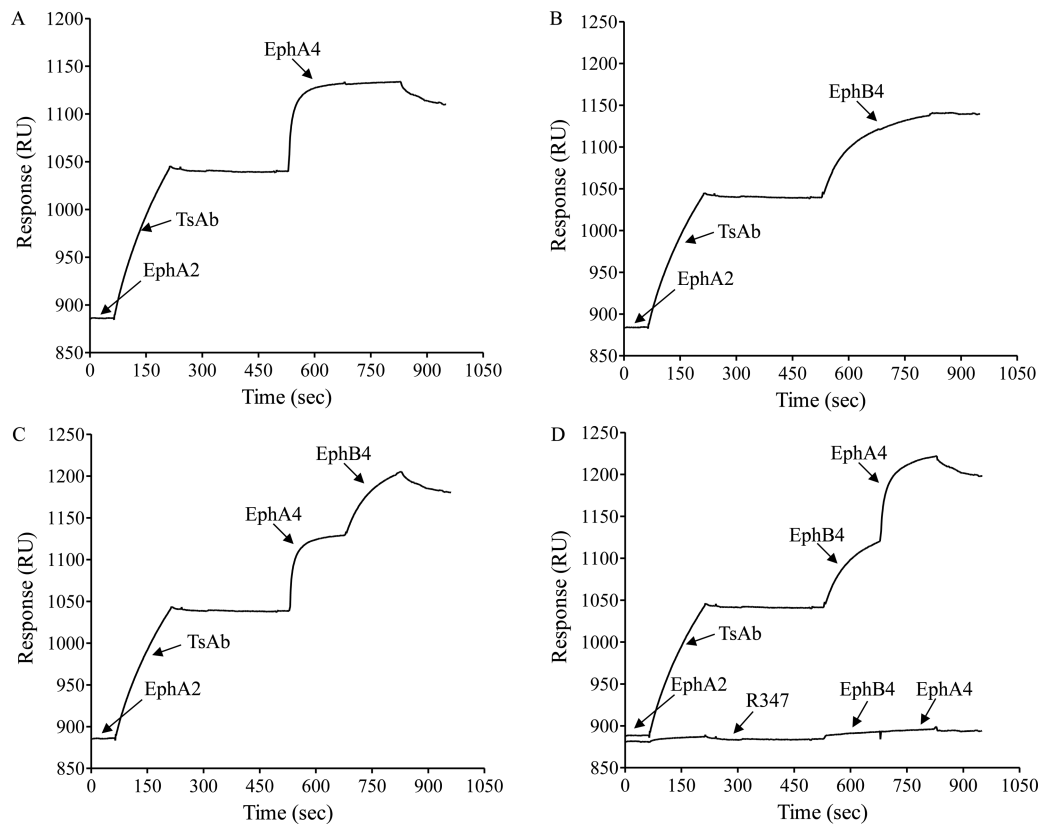
Figure 4. Cuncurrent binding of the trispecific to antigens using BIAcore. In these experiments EphA2 was immobilized on the BIAcore censor chip. Simultaneous binding of the trispecific (TsAb) to EphA2 and EphA4 (A) and to EphA2 and EphB4 (B). Concurrent binding to the three antigens (C,D). The trispecific antibody binds to its three antigens regardless of the sequence of antigen used, and the binding to antigens is specific since there is no detectable binding when the isotype control antibody (R347) is used (D).

Figure 5. Internalization analysis of the trispecific antibody. Time course of receptor mediated internalization of the (A) negative control R347, (B) anti-EphA2, and (C) trispecific antibodies. The antibodies were detected using AlexaFluor488 (fluorescent green color) labeled goat-γ-human IgG antibody. The cell nuclei were stained with DAPI. Images were analyzed by confocal laser-scanning microscopy. This experiment showed that the trispecific antibody efficiently internalizes into PC-3 prostate adenocarcinoma cells.
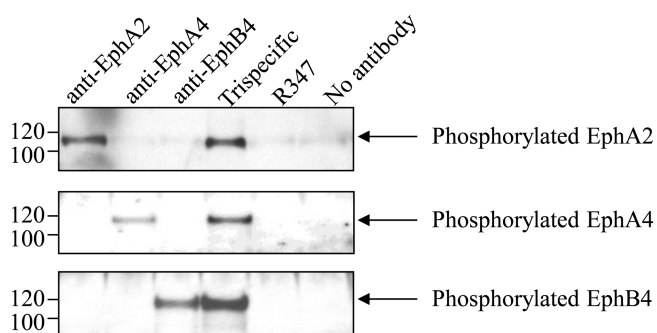
Figure 6. Induction of receptor phosphorylation by the trispecific antibody. MIA PaCa-2 cells were incubated with the trispecific and parental antibodies as schematically shown. An isotype negative antibody (R347) and no antibody treatments were included as negative controls. After incubation the cells were lysed, and phosphorylated EphA2, EphA4, and EphB4 were immunoprecipitated using receptor specific antibodies. Western blots were probed with antiphosphotyrosine HRP antibody and developed using enhanced chemiluminescence (ECL). The respective phosphorylated EphA2, EphA4, and EphB4 are schematically labeled. The molecular weights are reported in KDa.

of receptor mediated internalization. We did not detect internalization in MIA PaCa-2 cells using the negative control antibody R347 (Figure 5A). This data confirms that the trispecific antibody is efficiently internalized *in vitro* similarly to its anti-EphA2 parental antibody.

Receptor Phosphorylation by the Trispecific Antibody. To identify intracellular tyrosine phosphorylation of EphA2, EphA4, and EphB4 receptors mediated by the trispecific antibody binding to the extracelluar domains of the reseptors, MIA PaCa-2 cells were incubated with the trispecific antibody,

parental antibodies, and negative R347 control antibody (Figure 6). Receptor phosphorylation was observed after 30 min at 37 °C by receptor-specific antibody immunopurification followed by antiphospotyrosine detection. As seen in Figure 6, the trispecific antibody was able to induce tyrosine phosphorylation of all three receptors. These results suggest that the trispecific antibody is able to induce receptor activation in a manner similar to agonistic antibodies (i.e., mimic the action of endogenous ligands).

***In Vitro* and *in Vivo* Receptor Degradation Induced by the Trispecific Antibody.** Receptor degradation assays were carried out in order to determine if the trispecific antibody induces degradation of its target receptors both *in vitro* and *in vivo*. PC-3 cells, which express EphB4 and EphA2, were chosen because of their ability to proliferate into tumors upon injection in nude mice. Unfortunately, PC-3 cells do not express EphA4 and therefore could not be assayed for degradation of this receptor. Although MIA PaCa-2 cell lines do express EphA4, EphA2, and EphB4, as described for the *in vitro* receptor phosphorylation, these cells could not be used for the *in vivo* receptor degradation assays due to their low and variable tumor growth rate. Upon *in vitro* incubation of PC-3 cells with the trispecific antibody, both EphB4 (Figure 7A) and EphA2 (Figure 7B) are efficiently degraded and even better than the individual anti-EphA2 and anti-EphB4 parental antibodies. Next, we asked whether the trispecific antibody induces degradation of its target receptors in an *in vivo* tumor model system following systemic administration. It is important to point out that in order to induce *in vivo* receptor degradation the trispecific antibody must not only reach the tumor site but also penetrate into the tumor. Successful *in vivo* EphA2 and EphB4 degradation was verified by inoculating PC-3 cells into nude mice and determining the level
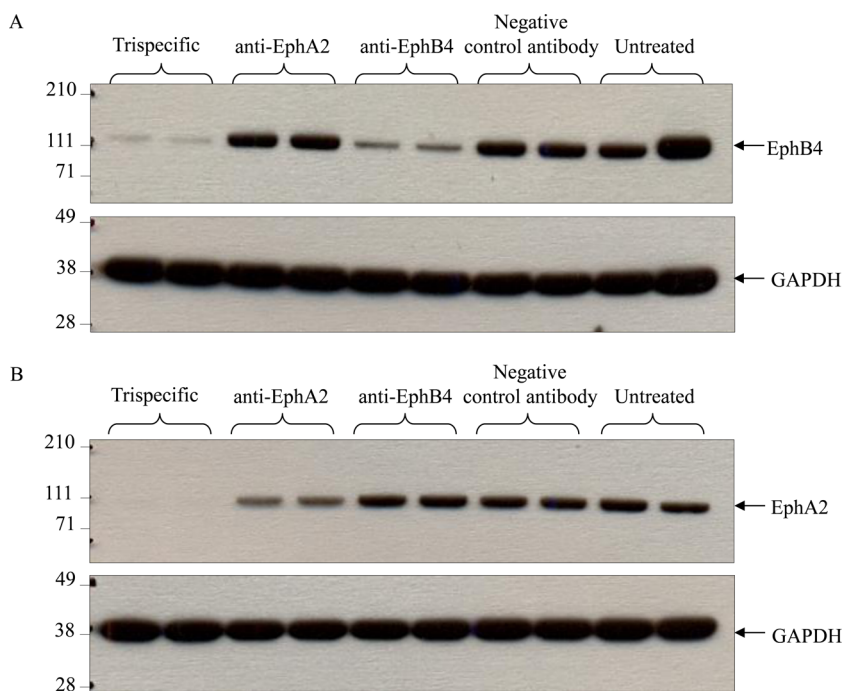
Figure 7. *In vitro* degradation of EphB4 and EphA2 in PC-3 cells by the trispecific antibody. The cells were treated with the trispecific or control antibodies (anti-EphA2, anti-EphB4, negative control R347 antibody or untreated) at 67 nM, as schematically shown. Trispecific and control antibodies were incubated with PC-3 cells for 4 h for EphB4 degradation (A) and 24 h for EphA2 degradation (B). Western blots were probed with anti-EphA2, anti-EphB4, and anti-GAPDH antibodies. The positions of EphB4, EphA2, and GAPDH (glyceraldehyde 3-phosphate dehydrogenase) are schematically shown. The molecular weights are reported in KDa.
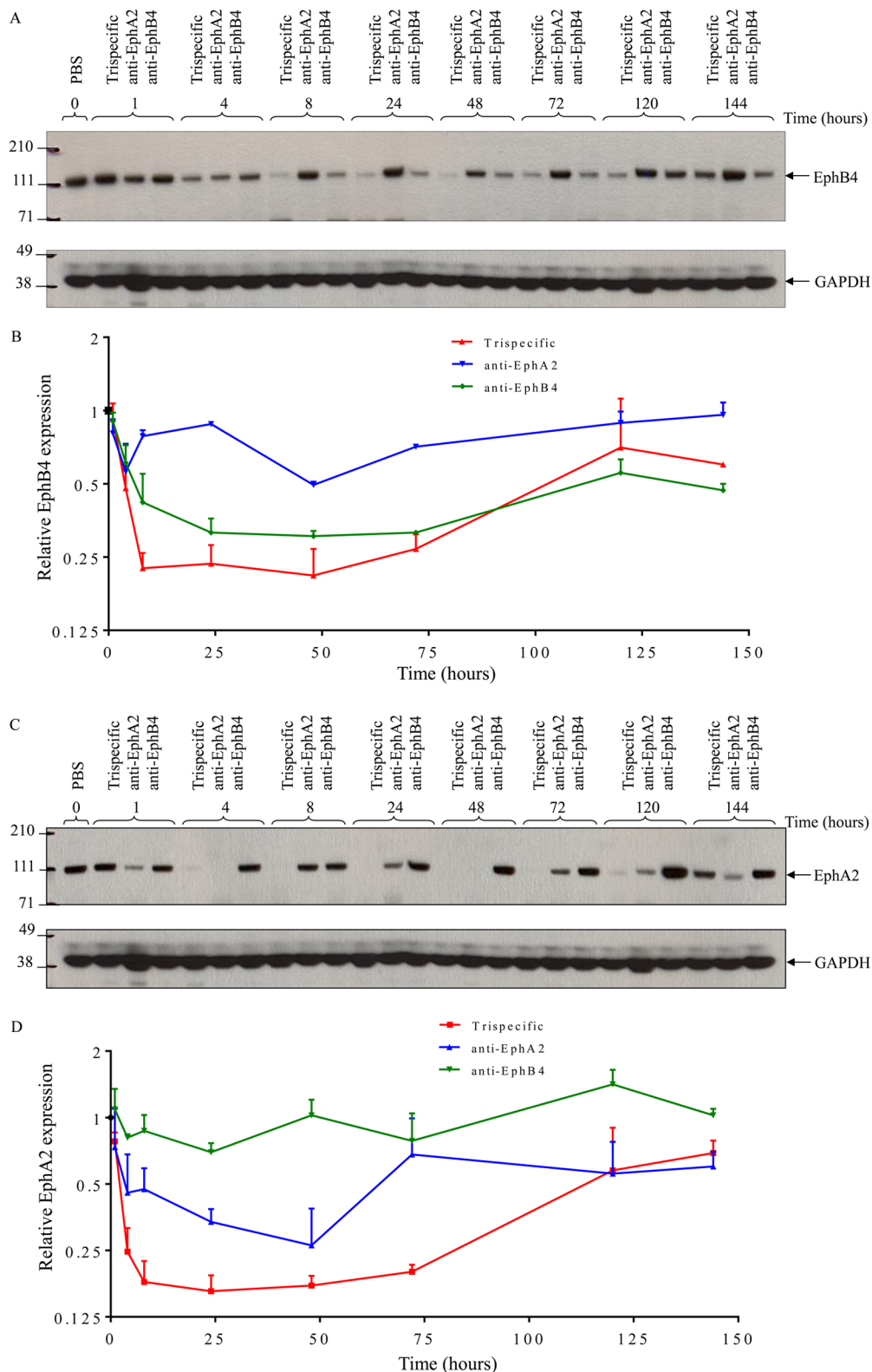
Figure 8. *In vivo* time course degradation of EphB4 and EphA2 in PC-3 tumor-bearing nude mice dosed with the trispecific, anti-EphA2, or anti-EphB4 antibody. Tumor lysates were analyzed by Western blot for EphB4 (A) and EphA2 (C) protein expression. GAPDH (glyceraldehyde 3-phosphate dehydrogenase) was used as control. The normalized densitometry values were plotted as mean of relative EphB4 (B) or EphA2 (D) expression using GraphPad Prism software. The molecular weights are reported in KDa.

of EphA2 and EphB4 expression upon trispecific or parental antibody treatment. As seen in Figure 8, both EphB4 and EphA2 are efficiently degraded by the trispecific antibody better than the respective parental anti-EphA2 and anti-EphB4 antibodies.

A possible explanation for the better *in vitro* and *in vivo* degradation is the fact that the trispecific antibody, designed to simultaneously engage three different antigens, may be able to efficiently promote clustering of different receptors at the cell

surface (better than the individual parental antibodies), thus improving efficiency of internalization and degradation.[30]

Pharmacokinetic Analysis of the Trispecific Antibody. Pharmacokinetic analyses of the trispecific antibody and its parental anti-EphA2 and anti-EphB4 antibodies were carried out using PC-3 tumor-bearing nude mice. The plasma concentration of the trispecific and parental antibodies were measured by ELISA at specific time points. As shown in Figure 9, the trispecific
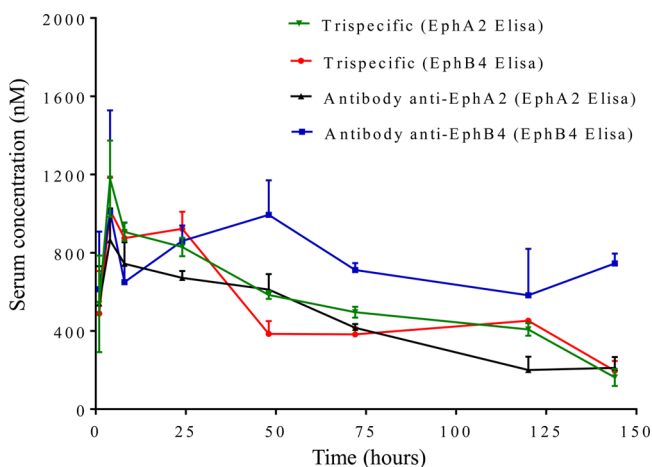
Figure 9. Trispecific antibody pharmacokinetic analysis in PC-3 tumor-bearing nude mice. Serum samples were analyzed for the presence of the trispecific antibody (green and red curves), parental anti-EphA2 antibody (black curve), or parental anti-EphB4 (blue curve) antibody using EphA2 and EphB4 binding ELISA. The levels of trispecific antibody in tumor-bearing nude mice are comparable to its respective parental antibodies.

antibody was still detectable at 144 h (6 days) postdosing with either EphA2 or EphB4 specific ELISA. In addition, the levels of plasma concentration of trispecific antibody were comparable with the levels of the individual parental antibodies. These data suggest that the circulation of the trispecific antibody in an *in vivo* tumor model system is similar to its respective parental antibodies, indicating the trispecific antibody is stable *in vivo*.

■ DISCUSSION

Overexpression of Ephs and ephrins contributes to tumor development by promoting tumor progression and metastasis. Thus, a specific blockade of Ephs/ephrins signaling pathways using antibody therapeutics could be an effective anticancer therapy. Among the Ephs receptors, EphA2, EphA4, and EphB4 appear to be overexpressed in a large number of tumors including breast, prostate, lung, and colon. Inhibition of EphA2-, EphA4-, and EphB4-mediated signal transduction may represent a reasonable approach for antitumor intervention. Monoclonal antibodies developed to target specific receptors expressed preferentially on tumor cells are approved for clinical use. Moreover, a number of recent reports[18−24,31−35] suggest that using a combination of monoclonal antibodies (i.e., a cocktail of two or more antibodies) to target different receptors or different epitopes on the same receptor have superior therapeutic efficacy over single antibody treatment. We believe that an efficient therapeutic approach for cancer therapy would be the simultaneous targeting of EphA2, EphA4, and EphB4 by using a recombinant trispecific antibody.

We developed a trispecific antibody targeting EphA2, EphA4, and EphB4 receptors and investigated whether simultaneously

targeting these three receptors would have a superior activity over single antibodies both *in vitro* and *in vivo*.

The trispecific antibody we designed consists of a full-length anti-EphA2 antibody followed by a diabody structure, comprising the V-domains of the anti-EphA4 and anti-EphB4 antibodies. We believe that this design is a generally applicable approach to develop hexavalent, trispecific, Ig-like molecules with considerable therapeutic potential. The trispecific antibody contains the complete human Fc region to maintain Fc functions, like effector functions and half-life, similar to traditional antibodies.

The trispecific antibody was expressed in mammalian cells and purified using the traditional protein A affinity chromatography. As demonstrated by analytical centrifugation, the purified trispecific antibody is monodisperse in solution with minimal aggregates. Differential scanning calorimetry analysis demonstrated transition temperatures of the trispecific antibody similar to its parental antibodies. Both monodispersity and transition temperatures that resemble those of the parental antibodies indicate the trispecific antibody has good biochemical and biophysical properties, which are acceptable for pharmaceutical development.

ELISA binding assay demonstrated the trispecific binds to its respective antigens or pair of antigens concurrently. BIAcore analysis revealed that the trispecific was capable of binding concurrently to three antigens, indicating that each domain independently binds to its cognate antigen. FACS experiments also confirmed that the trispecific antibody binds to its cognate targets expressed on carcinoma cells.

The concurrent binding of the trispecific to more than one target resulted in improved agonistic activity of the trispecific antibody over its respective parental antibodies as shown by increased receptor phosphorylation, internalization, and degradation both *in vitro* and *in vivo*. Unfortunately, the increased agonistic activity did not translate into enhanced antitumor activity over parental antibodies (data not shown), suggesting no direct correlation between agonistic activity and antitumor potency as reported by Kiewlich et al.[36] However, antibody mediated receptor internalization and subsequent degradation are applicable to antibody drug conjugates, which warrant the use of the trispecific antibody as an efficient vehicle to deliver anticancer small molecule drugs to tumors.

Simultaneous evaluation of PK and PD from a single intraperitoneal dose of antibodies showed a direct correlation between trispecific antibody exposure and EphA2 or EphB4 degradation. Complete receptor degradation was observed at antibody concentrations above ∼400 nM, and as antibody levels dropped at later time-points (120 h and later) due to time-dependent antibody elimination, receptor levels were observed to increase. Presumably, multidosing could extend receptor degradation exposure levels.

Lastly, we investigated serum circulation of the trispecific antibody and showed that the trispecific antibody has similar exposure to its respective parental antibodies following single dose administration in nude mice.

■ CONCLUSION

Multispecific biologics, like the trispecific antibody described herein, offer functionalities and targeting mechanisms unattainable with a single antibody or a mixture of two or more antibodies including improved tissue specific targeting through avidity, delivery of toxins, and receptor activation.

The trispecific antibody designed and characterized in this study provides a molecular scaffold to generate biologic drugs

that may be used to concurrently target three antigens, thereby broadening the spectrum of targeted therapeutics in oncology. In addition, combining three distinct binding functions into one trispecific antibody may provide a simple manufactural option over the mixture of individual antibodies.

■ ASSOCIATED CONTENT

ⓢ Supporting Information

The Supporting Information is available free of charge on the ACS Publications website at DOI: 10.1021/acs.molpharmaceut.5b00268.

> Schematic representation of the domains and their linear arrangement of the trispecific antibody; cartoon representation of the trispecific antibody; and amino acid sequence of the light and heavy chains of the trispecific antibody (PDF)

■ AUTHOR INFORMATION

Corresponding Authors

*E-mail: dimasin@medimmune.com.
*E-mail: gaoc@medimmune.com.

Author Contributions

Conceived and designed the experiments: N.D., C.G. Performed the experiments: N.D., R.F., R.W., L.X., C.H. Analyzed the data: all authors. Wrote the paper: N.D. Provided critical review of the paper: all authors. Provided scientific guidance: C.G., H.W.

Notes

The authors declare the following competing financial interest(s): The authors are employees of MedImmune and may own AstraZeneca stocks or stock options.

■ REFERENCES

(1) Al-Ejeh, F.; Offenhäuser, C.; Lim, Y. C.; Stringer, B. W.; Day, B. W.; Boyd, A. W. Eph family co-expression patterns define unique clusters predictive of cancer phenotype. *Growth Factors* **2014**, *32*, 254−264.

(2) Boyd, A. W.; Bartlett, P. F.; Lackmann, M. Therapeutic targeting of EPH receptors and their ligands. *Nat. Rev. Drug Discovery* **2014**, *13*, 39−62.

(3) Gale, N. W.; Holland, S. J.; Valenzuela, D. M.; et al. Eph receptors and ligands comprise two major specificity subclasses and are reciprocally compartmentalized during embryogenesis. *Neuron* **1996**, *17*, 9−19.

(4) Surawska, H.; Ma, P. C.; Salgia, R. The role of ephrins and Eph receptors in cancer. *Cytokine Growth Factor Rev.* **2004**, *16*, 419−433.

(5) Ireton, R. C.; Chen, J. EphA2 receptor tyrosine kinase as a promising target for cancer therapeutics. *Curr. Cancer Drug Targets* **2005**, *5*, 149−157.

(6) Iiizumi, M.; Hosokawa, M.; Takehara, A.; Chung, S.; Nakamura, T.; Katagiri, T.; Eguchi, H.; Ohigashi, H.; Ishikawa, O.; Nakamura, Y.; Nakagawa, H. EphA4 receptor, overexpressed in pancreatic ductal adenocarcinoma, promotes cancer cell growth. *Cancer Sci.* **2006**, *97*, 1211−1216.

(7) Ferguson, B. D.; Tretiakova, M. S.; Lingen, M. W.; Gill, P. S.; Salgia, R. Expression of the EPHB4 receptor tyrosine kinase in head and neck and renal malignances - implications for solid tumors and potential for therapeutic inhibition. *Growth Factors* **2014**, *32*, 202−206.

(8) Ferguson, B. D.; Liu, R.; Rolle, C. E.; Tan, Y. H.; Krasnoperov, V.; Kanteti, R.; Tretiakova, M. S.; Cervantes, G. M.; Hasina, R.; Hseu, R. D.; Iafrate, A. J.; Karrison, T.; Ferguson, M. K.; Husain, A. N.; Faoro, L.; Vokes, E. E.; Gill, P. S.; Salgia, R. The EphB4 receptor tyrosine kinase promotes lung cancer growth: a potential novel therapeutic target. *PLoS One* **2013**, *7*, e67668.

(9) Liu, R.; Ferguson, B. D.; Zhou, Y.; Naga, K.; Salgia, R.; Gill, P. S.; Krasnoperov, V. EphB4 as a therapeutic target in mesothelioma. *BMC Cancer* **2013**, *13*, 269.

(10) Hasina, R.; Mollberg, N.; Kawada, I.; Mutreja, K.; Kanade, G.; Yala, S.; et al. Critical role for the receptor tyrosine kinase EPHB4 in esophageal cancers. *Cancer Res.* **2013**, *73*, 184−194.

(11) Kumar, S. R.; Singh, J.; Xia, G.; Krasnoperov, V.; Hassanieh, L.; Ley, E. J.; Scehnet, J.; Kumar, N. G.; Hawes, D.; Press, M. F.; Weaver, F. A.; Gill, P. S. Receptor tyrosine kinase EphB4 is a survival factor in breast cancer. *Am. J. Pathol.* **2006**, *169*, 279−293.

(12) Kumar, S. R.; Masood, R.; Spannuth, W. A.; Singh, J.; Scehnet, J.; Kleiber, G.; Jennings, N.; Deavers, M.; Krasnoperov, V.; Dubeau, L.; Weaver, F. A.; Sood, A. K.; Gill, P. S. The receptor tyrosine kinase EphB4 is overexpressed in ovarian cancer, provides survival signals and predicts poor outcome. *Br. J. Cancer* **2007**, *96*, 1083−1091.

(13) Yang, N. Y.; Pasquale, E. B.; Owen, L. B.; Ethell, I. M. The EphB4 receptor-tyrosine kinase promotes the migration of melanoma cells through Rho-mediated actin cytoskeleton reorganization. *J. Biol. Chem.* **2006**, *281*, 32574−3286.

(14) Rougier, P.; Lepère, C. Metastatic Colorectal Cancer: First- and Second-Line Treatment in 2005. *Semin. Oncol.* **2005**, *32*, 15−20.

(15) Hurwitz, H. Integrating the anti-VEGF-A humanized monoclonal antibody bevacizumab with chemotherapy in advanced colorectal cancer. *Clin. Colorectal Cancer* **2004**, *4*, S62−S68.

(16) Hurwitz, H. I.; Fehrenbacher, L.; Hainsworth, J. D.; Heim, W.; Berlin, J.; Holmgren, E.; Hambleton, J.; Novotny, W. F.; Kabbinavar, F. Bevacizumab in combination with fluorouracil and leucovorin: an active regimen for first-line metastatic colorectal cancer. *J. Clin. Oncol.* **2005**, *23*, 3502−3508.

(17) Kabbinavar, F. F.; Hambleton, J.; Mass, R. D.; Hurwitz, H. I.; Bergsland, E.; Sarkar, S. Combined analysis of efficacy: the addition of bevacizumab to fluorouracil/leucovorin improves survival for patients with metastatic colorectal cancer. *J. Clin. Oncol.* **2005**, *23*, 3706−3712.

(18) Kabbinavar, F. F.; Schulz, J.; McCleod, M.; Patel, T.; Hamm, J. T.; Hecht, J. R.; Mass, R.; Perrou, B.; Nelson, B.; Novotny, W. F. Addition of bevacizumab to bolus fluorouracil and leucovorin in first-line metastatic colorectal cancer: results of a randomized phase II trial. *J. Clin. Oncol.* **2005**, *23*, 3697−3705.

(19) Tolstrup, A. B.; Frandsen, T. P.; Bregenholt, S. Development of recombinant human polyclonal antibodies for the treatment of complex human diseases. *Expert Opin. Biol. Ther.* **2006**, *9*, 905−912.

(20) Uno, T.; Takeda, K.; Kojima, Y.; Yoshizawa, H.; Akiba, H.; Mittler, R. S.; et al. Eradication of established tumors in mice by a combination antibody-based therapy. *Nat. Med.* **2006**, *12*, 693−698.

(21) Leonard, J. P.; Coleman, M.; Ketas, J.; Ashe, M.; Fiore, J. M.; Furman, R. R.; et al. Combination antibody therapy with epratuzumab and rituximab in relapsed or refractory non-Hodgkin's lymphoma. *J. Clin. Oncol.* **2005**, *23*, 5044−5051.

(22) Strauss, S. J.; Morschhauser, F.; Rech, J.; Repp, R.; Solal-Celigny, P.; Zinzani, P.; et al. Multicenter phase II trial of immunotherapy with the humanized anti-CD22 antibody, epratuzumab, in combination with rituximab, in refractory or recurrent non-Hodgkin's lymphoma. *J. Clin. Oncol.* **2006**, *24*, 3880−3886.

(23) Ye, D.; Mendelsohn, J.; Fan, Z. Augmentation of a humanized anti-HER2 mAb 4D5 induced growth inhibition by a human-mouse chimeric anti-EGF receptor mAb C225. *Oncogene* **1999**, *18*, 731−738.

(24) Kawaguchi, Y.; Kono, K.; Mimura, K.; Mitsui, F.; Sugai, H.; Akaike, H.; Fujii, H. Targeting EGFR and HER-2 with cetuximab- and trastuzumab-mediated immunotherapy in oesophageal squamous cell carcinoma. *Br. J. Cancer* **2007**, *97*, 494−501.

(25) Farid, S. S. Process economics of industrial monoclonal antibody manufacture. *J. Chromatogr. B: Anal. Technol. Biomed. Life Sci.* **2007**, *848*, 8−18.

(26) Spiess, C.; Carter, P. J. Alternative molecular formats and therapeutic applications for bispecific antibodies. *Mol. Immunol.* **2015**, DOI: 10.1016/j.molimm.2015.01.003.

(27) Dimasi, N.; Gao, C.; Fleming, R.; Yao, X. T.; Shirinian, L.; Kinier, P.; Herren, W. The design and characterization of polyspecific antibodies for simultaneous targeting of multiple disease mediators. *J. Mol. Biol.* **2009**, *393*, 672−692.

(28) Bezabeh, B., Fleming, R., Coffman, K., Leow, C. C., Gibson, N., Wilson, S., Stover, C. K., Wu, H., Gao, C., Dimasi, N. Design and characterization of a novel tetravalent bispecific antibody. Submitted.

(29) Schuck, P. Size-distribution analysis of macromolecules by sedimentation velocity ultracentrifugation and lamm equation modeling. *Biophys. J.* **2000**, *78*, 1606−1619.

(30) Friedman, L. M.; Rinon, A.; Schechter, B.; Lyass, L.; Lavi, S.; Bacus, S. S.; et al. Synergistic down-regulation of receptor tyrosine kinases by combinations of mAbs: implications for cancer immunotherapy. *Proc. Natl. Acad. Sci. U. S. A.* **2005**, *102*, 1915−1920.

(31) Loisel, S.; André, P. A.; Golay, J.; Buchegger, F.; Kadouche, J.; Cérutti, M.; Bologna, L.; Kosinski, M.; Viert, D.; Bischof Delaloye, A.; Berthou, C.; Mach, J. P.; Boumsel, L. Antitumour effects of single or combined monoclonal antibodies directed against membrane antigens expressed by human B cells leukaemia. *Mol. Cancer* **2011**, *10*, 42.

(32) Nejatollahi, F.; Jaberipour, M.; Asgharpour, M. Triple blockade of HER2 by a cocktail of anti-HER2 scFv antibodies induces high antiproliferative effects in breast cancer cells. *Tumor Biol.* **2014**, *35*, 7887−7895.

(33) Pedersen, M. W.; Jacobsen, H. J.; Koefoed, K.; Hey, A.; Pyke, C.; Haurum, J. S.; Kragh, M. Sym004: a novel synergistic anti-epidermal growth factor receptor antibody mixture with superior anticancer efficacy. *Cancer Res.* **2010**, *70*, 588−597.

(34) Pedersen, M. W.; Jacobsen, H. J.; Koefoed, K.; Dahlman, A.; Kjaer, I.; Poulsen, T. T.; Meijer, P. J.; Nielsen, L. S.; Horak, I. D.; Lantto, J.; Kragh, M. Targeting Three Distinct HER2 Domains with a Recombinant Antibody Mixture Overcomes Trastuzumab Resistance. *Mol. Cancer Ther.* **2015**, *14*, 669.

(35) Scheuer, W.; Friess, T.; Burtscher, H.; Bossenmaier, B.; End, J.; Hasmann, M. Strongly enhanced antitumor activity of trastuzumab and pertuzumab combination treatment on HER2-positive human xenograft tumor models. *Cancer Res.* **2009**, *69*, 9330−9336.

(36) Kiewlich, D.; Zhang, J.; Gross, C.; Xia, W.; Larsen, B.; Cobb, R. R.; Biroc, S.; Gu, J. M.; Sato, T.; Ligh, D. R.; Heitner, T.; Willuda, J.; Vogel, D.; Monteclaro, F.; Citkowicz, A.; Roffler, S. R.; Zajchowski, D. A. Anti-EphA2 antibodies decrease EphA2 protein levels in murine CT26 colorectal and human MDA-231 breast tumors but do not inhibit tumor growth. *Neoplasia* **2006**, *8*, 18−30.